PSFC/JA-03-02

Superconducting options for final optics magnets for the Heavy Ion Driver in Inertial Fusion Energy

L. Bromberg[1]
and

the ARIES team
January 20, 2003

[1] MIT Plasma Science and Fusion Center

Submitted for publication to Journal of Fusion Energy

Work supported by US Department of Energy Office of Transportation Technologies.

Superconducting options for final optics magnets for the Heavy Ion Driver in Inertial Fusion Energy

L. Bromberg
MIT Plasma Science and Fusion Center

and the ARIES team

Abstract

The environment close to the chamber in inertial fusion confinement imposes severe constrains on magnets used for final focusing magnets needed for the heavy ion driver. Space is at a premium, requiring close proximity of adjacent magnets, making magnet integration imperative. In addition, the high radiation flux and heating rate imposes requirements that are as stringent as in magnetic fusion. In this paper, the options for final focusing magnet topologies are described. Implication of using both high Tc and conventional low temperature superconductors are investigated. The use of HTS material may offer an opportunity for a fundamentally different approach to magnet construction leading to either lower cost or reduced maintenance.

I. Introduction

The final optics magnets for the Heavy Ion Driver for inertial fusion present design challenges. The magnets are quadrupoles, used for final focusing of beam arrays. Because of space requirements, it is optimal to pack them in as tight an array as possible. In this configuration, adjacent magnets interact with each other, electromagnetically, structurally and thermally.

Because of the close contact between them, it is interesting to explore the design concepts that exploit this feature. Quadrupole magnet arrays can be optimized beyond the assembly of the array from individually optimized quadrupole magnets. It is the purpose of this paper to explore this optimization.

The issues in the design of the magnets have to do with the high radiation fields present in the magnets, affecting the superconducting properties of the conductor, the properties of the normal material stabilizer/quench protector, the insulation and the cooling. The radiation characteristics are also different from those in magnetic fusion, because of the pulsed nature of the radiation. This effect has impact on the radiation limit for the insulator.

The choice of superconductor has effect of the characteristics of the magnet array. While low Tc superconductors are more developed, the prospect of high Tc offers advantages in the design, manufacturing and operation of final optic magnets for IFE.

In this paper, the design options for final optic magnet arrays are discussed. The restrictions imposed on optimized, aggressive high Tc quadrupole final optic magnets operating at elevated temperatures are discussed. A comparison is then made with optimized quadrupoles that use low Tc materials.

II. Quadrupole array design options.

The design of quadrupole arrays, especially those that need q high density of quadrupoles, represents different requirements than those when designing individual quadrupoles {Faltens]. The latter ones have an extensive literature, due to their use in particle physics experiments. Low temperature superconducting quadrupole arrays have been investigated, including cryogenic, structural and superconducting issues for a particular case [Meinke]. In this section, the options for the design of quadrupole magnet arrays are generalized.

a. Magnetic field calculations

The scalar potential description of the magnetic field is

$$\boldsymbol{B} = -\square\ \square,$$

where **B** is the magnetic field and Φ the scalar potential. This description is useful when the volume is void of currents, when it can be shown that the above scale potential has to satisfy LaPlace's equation,

$$\nabla^2 \Phi = 0.$$

The design of quadrupole arrays requires the application of the boundary conditions. However, it is instructive to solve (2) first, and the find the boundary conditions that apply for the different solutions.

The solution of LaPlace's equation with appropriate poloidal angle dependence in cylindrical coordinates is

$$\Phi = \Sigma (\sin (m\theta) (A_{1,m} r^m + B_{1,m} r^{-m}) + \cos (m\theta) (A_{2,m} r^m + B_{2,m} r^{-m}))$$

where θ is the poloidal angle and r is in the radius from the center of the cell. The sum is for m > 0. Since the solution needs to be well behaved at r = 0, only solutions with $B_{1,m} = B_{2,m} = 0$ are allowed.

For a quadrupole field structure, m = 2, and therefore the solution for the scalar potential is

$$\Phi = A_1 r^2 \sin (2\theta) + A_2 r^2 \cos (2\theta)$$

The solution with $A_1 = 0$ will be referred to as the cosine quadrupole, while the solution with $A_2=0$ will be referred to as the sine quadrupole. There could be linear superposition of the two solutions, but in practice only one or the other are of interest.

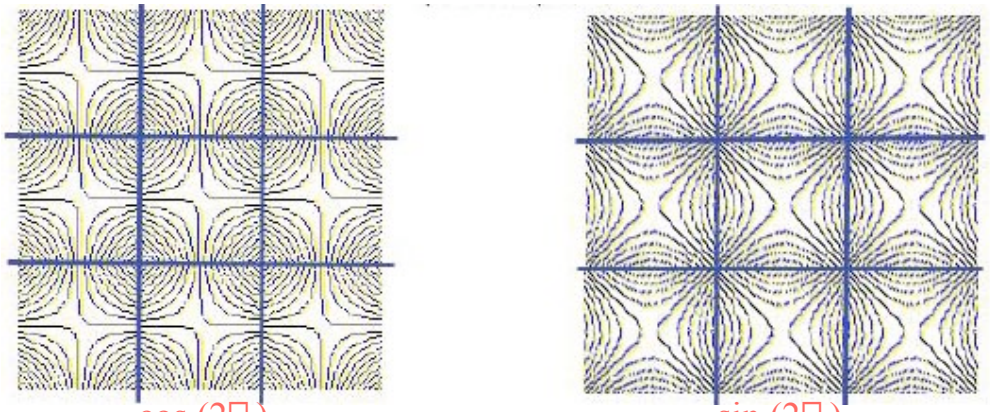

Figure 1. Field profiles for sine and cosine quadrupole arrays

Figure 1 shows the field profile for the quadrupole array for both the sine and cosine solutions. In the sine quadrupole case, the magnetic field in the region close to the to the boundary has substantial components parallel to the boundary between cells, while in the cosine quadrupole case the magnetic field is only

perpendicular to this boundary. Again, cells need to be located next to each other because of space limitation at the location of the final focusing magnets.

It should be noted that the heavy ion beam is elongated/compressed in the direction perpendicular to the field of the quadrupole. Therefore, the cosine quadrupole may offer geometrical advantages. In the case of the cosine quadrupole, the axis of the ellipse formed by the beam cross section is in the diagonal of the cell, while in the case of the sine quadrupole, it is in the direction normal to the boundaries of the cell. For circular beams there is no net effect, but for the case of elliptical beam.

It the beam apertures are made circular, the closest packing can be obtained not by using arrangement in a square matrix, as shown in Figure 1 but instead in a hexagonal, honeycomb-like pattern (m = 3). However, since the field pattern is "square" looking (m=2), the use of a square pattern is a more natural one, and results in a better match better between the required field structure and the magnet arrangement.

Because of the different field profile in the cell, the current density at the boundary between cells is different for the cosine and sine quadrupoles. Using symmetry as shown in Figure 1 it is straightforward to calculate the surface current density required to produce the magnetic field. The surface current density K is determined by

$$K = \Delta B/\mu_0$$

where $\Delta B = (B_1 - B_2)$, where B_1 and B_2 are the values of the magnetic fields parallel to the surface at opposite sides of the boundary. The field perpendicular to the surface is continuous, due to the divergence free nature of magnetic fields. The surface current density is in the direction perpendicular of the fields, directed along the surface and aligned with the main axis of the focusing magnet.

For the sine quadrupoles, the surface current density is given by

$$|K_{sine,x\text{-}wall}| = 4\ A\ x\ /\mu_o \quad \text{for } -a < x < a$$

on the x-wall and

$$|K_{sine,y\text{-}wall}| = 4\ A\ y\ /\mu_o \quad \text{for } -a < y < a$$

on the y-wall. Here a is the half width of the cell, and A is a constant. The current therefore reverses on each face. The current density is not uniform, but increases linearly starting at the center of each face, but in opposite directions.

For the cosine quadrupole, the current density in each face is uniform, given by

$$|K_{cosine}| = 4\ A\ a\ /\mu_o$$

In this case, the net current in each face of the quadrupole is not zero, and therefore the current needs to be balanced by returning the current that flows in one face through the adjacent faces. The current distribution for the cosine and sine quadrupoles arrays are shown in Figure 2.

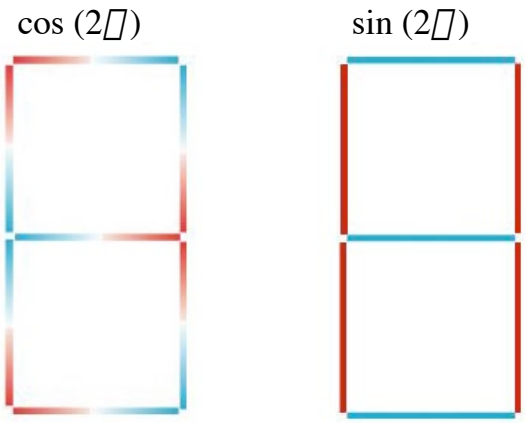

Figure 2. Current distribution in planar cosine and sine quadrupoles. Different color indicates different current direction.

In both the sine and cosine quadrupoles, the total magnetic field is given by

$$| B | = 2 A \ r$$

and the gradient of the magnetic field magnitude is

$$| B |' = 2 A$$

b. Force considerations

In this section, the forces in the quadrupole arrays for the final optics magnets will be described. Because of symmetry, it is straightforward to show that the forces are aligned along the cell boundaries, resulting only on in-plane loads. However, the in-plane loads can be transverse (perpendicular to the main axis of the plate) or longitudinal, along the axis of the plates.

The forces in the quadrupoles are complex, because of the ends. The longitudinal loads are exclusively generated by the quadrupole ends. They are also aligned on the planes of the cell boundaries. However, the longitudinal loads due to the ends are relatively small compared with the transverse ones, and will be ignored in the discussions below, which are meant more for scoping studies rather than detailed design.

The forces due to the axial current flowing in quadrupole arrays can be easily calculated, using the analytical solution for the planar quadrupole obtained in the previous section. For both sine and cosine quadrupoles, the integrated transversal force per unit length is given by

$$F = 4\ A^2\ a^3 / \mu_o$$

And the value of the associated transverse stresses is given by

$$\sigma = F/t$$

where t is the thickness of the structural plate.

Even though the force magnitudes are equal, there is a fundamental difference between the sine and the cosine quadrupoles. While the cosine quadrupole has a tensile load across the narrow dimension of the plane of the quadrupole, the sine quadrupole has a compressive load. The load support is not only determined by the intrinsic properties of the structural material (material strength), but also by buckling considerations.

It is possible to prevent tension in the structure for the case of the cosine quadrupole by preventing the loads path from going through the center of the plate (for example, by making a slit through the middle of the flat plate. In this case, the loads need to be reacted by the adjacent plate, which also has a force equal in magnitude but opposite in direction. As in the case of the sine quadrupole, care needs to be taken to prevent buckling of the plates when in compression.

The design requirements for the structural material also needs to meet strain limitations of the superconductor. To limit strain in SC to 0.2% (comparable to LTS), the maximum tensile stress in structure is ~500 MPa Compressive stresses are comparable, but in practice for our case are limited by buckling.

c. Stored Energy

In order to provide quench protection, required for low temperature superconductors, it is necessary to determine the stored magnetic energy in the quadrupoles. For both magnet topologies, with flat plates, the energy per quadrupole is given by

$$E = 16\ A^2\ a^4\ L\ /\ 3\ \mu_o$$

Here L is the length of the quadrupole. Typical numbers are about 200 kJ per magnet. An array of about 100 magnets would therefore store about 20 MJ. It may be possible to connect all the magnets in the array in a series configuration. Assuming 2500A conductor the dump time for 20 kV would be about several seconds. Because of this, it may be necessary to electrically divide the quadrupole array. This determines the amount of copper stabilizer required for the case of quench protection in low temperature superconductors.

d. Manufacturing consideration for planar quadrupole magnet arrays

The planar quadrupole magnets that are attractive for the final focusing magnets arrays have current density distributions that are different from that of conventional quadrupoles, as indicated above. Their manufacturing should be altered.

The options for manufacturing the planar elements that make up a quadrupole in an array are shown in Figure 2. For the case of the cosine quadrupoles, the magnet can be made from flat plates, one for each boundary between cells. These flat plates carry no net current. The plates can in introduced into a structural grid to provide appropriate positioning ("keying") of the individual flat plates. As indicated in the above section, the net load in the plates is zero (by symmetry), and the loads are all in the plate direction (resulting in no requirement of out-of-plane loads, that need to be supported by bending).

In contrast, the sine quadrupole has the current in the same direction in each plate. Therefore, the electrical requirements of net zero current in each element (so that the current in the leads can be small) indicate that a different approach must be taken. There are two ways to implement this solution, as shown in Figure 3a.The first one, each quadrupole is made of two sections, using 90 degree angle elements. In this manner, the current on one of the plates making the 90 degree angle element is returned in the other plate of the angle element. In this case, with two 90 degree angle elements per quadrupole as shown in Figure 3(a), the net forces in each of the plates are zero, by symmetry. Each angle of the plates, however, experiences large compressive stresses that need to be supported against buckling, as described above. In this case, the number of full-angle elements required in the quadrupole array is approximately the same as the number of quadrupoles in the array, since the elements are shared.

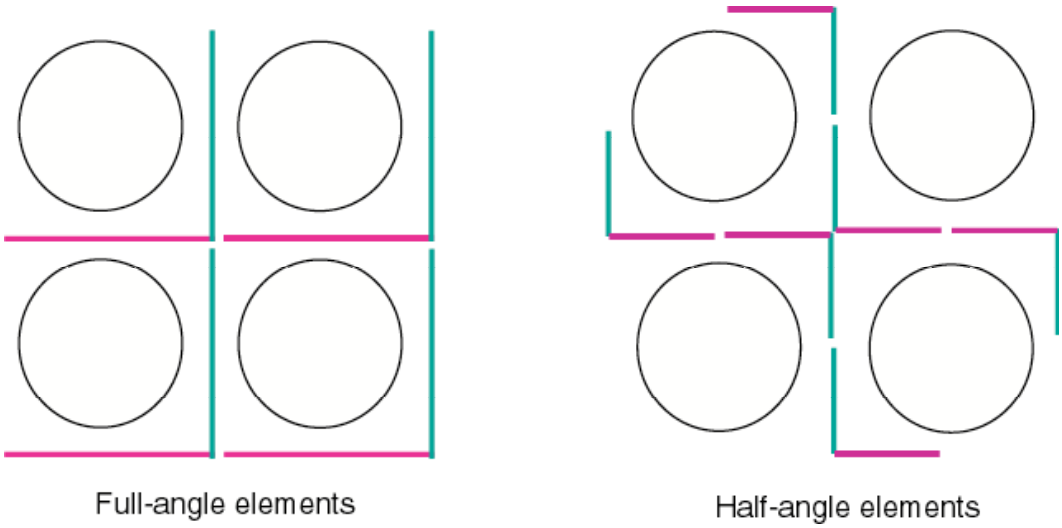

Figure 3. Options of sine quadrupole arrangement made of (a) full-angle elements (b) half-angle elements

An alternative method of implementing this geometry would involve making each quadrupole out of 4 separate half-angle segments, as shown in Figure 3b. In this case, each quadrupole magnet has 4 elements. In this case, although the fields are shared, it is necessary for each quadrupole to have four elements. The adjacent

quadrupoles need to have their own 90 degree angle elements as shown in Figure 3 b.

III. Design requirements for quadrupole magnet arrays.

Superconductors have four design requirements that that must be considered when they are used in nuclear applications. These are: survival of the insulation, the stabilizer and the superconductor under irradiation, and removal of nuclear heating. In this section, these requirements are summarized and their impact on the high temperature superconductor options reviewed.

a. Insulation

Organic insulators have substantially lower fluence life than inorganic insulators. This is because organic insulators are limited by chemical changes due to bond breaking, while for inorganic insulators the life is determined by swelling caused by gas generation by nuclear process or damage to the crystallographic structure of the material.

In organics, the bond breaking can be described in terms of g-values, or the number of radicals, atoms or bonds broken per 100 eV of absorbed energy. Since the mechanism for different types of irradiation are similar, the g-values from these different forms of radiation are comparable. Therefore, the relevant number for characterizing irradiation damage from neutrons, gammas and electrons are in terms of energy density dissipated in the material, or Grays. For organics, both neutrons and gammas cause damage, and fluence life limits are around 10^8 Grays, even in the absence of shear across the insulation.

The fluence limit for inorganic insulators is determined by swelling. For practical insulators the maximum irradiation ranges from 10^9 rads to 10^{12} Grays depending whether the insulator is in sheets or in powder form. The corresponding neutron fluence is 10^{24}-10^{27} neutrons/m^2.

For IFE final focusing magnets, because of the openings required for transmission of the beam, not only the radiation is, for a constant thickness shield, larger than for comparable MFE concepts, but the spectrum and the nature of the radiation is also different. Table 1 shows the neutron and gamma maximum insulator fluences assuming a machine with 40 full power years. Three places are shown for the ARIES-AT design, while the radiation to the insulator of the final focusing magnet is shown for varying thickness of the beam-flibe distance. Not only the values are much larger for the final focusing magnets than they are for ARIES-AT, but the ratio between gammas and neutrons is also very different. The gamma fluence is about a factor of 6 larger than the neutron fluence, while for ARIES-AT the neutron and gamma fluences are comparable. This is because of the lack of neutron capture materials that tend to decrease the neutron flux and the □-ray generation rate close to the magnets.

Table 1
Neutron, gamma and total fluences (in MGrays) for illustrative tokamak (ARIES-AT) and calculated for IFE final focus magnets, 40 FPY, polyimide insulation

		Neutrons	Gammas	Total
ARIES-AT				
	Inboard	41	33	74
	Divertor	31	26	57
	Outboard	50	320	370
IFE-Flibe				
	1 cm gap	380	2480	2860
	0 cm gap	100	600	700

Not only can the neutron/gamma distribution different between IFE and tokamak applications, but the dose rate is also extremely different. While for magnetic fusion applications the dose rate is nearly constant, for IFE the dose rate is pulsed, with very low duty cycle. The radiation pulse in IFE is less than 1 μsec while the pulse rate is about 10 times a second, the dose rate is 5 orders of magnitude larger than for MFE with equivalent average dose rates.

The effect of dose rate is unknown for the organics that are being considered now. For very high instantaneous dose rates, it is possible that the radicals/ions/atoms generated interact with each other due to their much higher density. It has been mentioned that damage to organic insulators is due to changes in chemistry. High dose rates results in large concentration of radicals generated in the radiation, which could recombine with each other (increasing gas generation). On the other hand the data from aging of irradiation indicates that lower radiation dose rates, the insulation damage is greater. [Chapiro]

Present day testing in TRIGA reactors result in a does rate of about 300 Gray/s. The average dose rate for aggressive IFE designs is on the order of 1 Gray/s, with an instantaneous dose of about 0.1 MGray/s. For comparison, the average dose rate for ARIES-AT is about 0.25 Gray/s. Therefore, the present testing rate is accelerated for magnetic fusion (by about a factor of 1000), but slow compared to the instantaneous dose rate in inertial fusion (by a factor of about 300).

From these discussions it is clear that the final focus magnets could benefit, although only slightly, from the use of inorganic insulation. Not only are the limits of this type of insulation higher than radiation resistant organic insulators, but inorganic insulators are not sensitive to gamma rays. Present day data on high performance organic insulators indicate the feasibility of utilizing organics up to a few times 100 MGrays. [Bittner]

b. Stability/quench protection

High temperature superconductors do not suffer from flux-jumping when operated at temperatures higher than about 10-20 K, because of the very high thermal capacity of the metals at these temperatures (about 2 orders of magnitude higher than at 4K). As a result, there is no need for a substantial fraction of normal conducting material, in contrast with LTS materials. The only normal conducting material required is whatever is needed to manufacture the superconductor. In the case of YBCO, it is a Ni tape. For BSCCO, the filaments are likely to be placed in a silver matrix.

The high thermal capacity of high Tc materials increases the difficulty of quench-detection, mainly because the quench-zone propagates very slowly in high-Tc superconductors. For active magnet protection, novel methods of quench protection and quench detection would be required for high-Tc superconductors at high temperatures. Since a very large source of energy is required to start a quench it is assumed that flux jumping and quenching do no occur. For the high-Tc design it is assumed that all of the stabilizer and quench protection normal conductor could in principle be eliminated from the coil.

For low temperature superconductors, the need for stabilizer and quench is required, and this material is included in the conductor. The radiation damage to the stabilizer/quench protector is assumed to be annealed with periodic warm up of the magnet during scheduled maintenance periods.

c. Superconductor

The properties of high-Tc materials which are of interest in fusion have been recently described, and will only be briefly reviewed in this paper [Bromberg 01, Schultz]. High temperature superconducting (HTS) materials are ceramic and therefore brittle in nature. The production of long lengths of wires or tapes suitable for winding magnets has limited the application of high-temperature superconductors. The solutions developed for manufacturing high performance A-15 superconductors (such as Nb_3Sn) are being used in the fabrication of HTS wires. In this paper, thick-film films (of $YBa_2Cu_3O_{7-x}$ compounds, referred as YBCO) are assumed. However, it should be mentioned that long length tapes made of this material have yet to be manufactured [Iijima, Maley]. Short sample properties will be assumed, with the hope that in the future the barriers for manufacturing of long lengths of thick tapes will be overcome.

The measurements of YBCO-123 performance at several temperatures as a function the magnetic field are shown in Figure 4 [Maley]. These results were obtained for highly textured tapes, and show the difference in the behavior of these highly anisotropic superconductors to magnetic fields that are applied either perpendicular or parallel to the main plane of the crystal. The performance of YBCO at liquid nitrogen temperature and 10 T is comparable to that of non-copper current density of Nb_3Sn superconductor, at 4 K and 0 T. Indeed, once the structure and stabilizer/quench protection is included in the Nb_3Sn designs, the average current density in the Nb_3Sn conductor is substantially lower than that for YBCO at elevated temperatures.

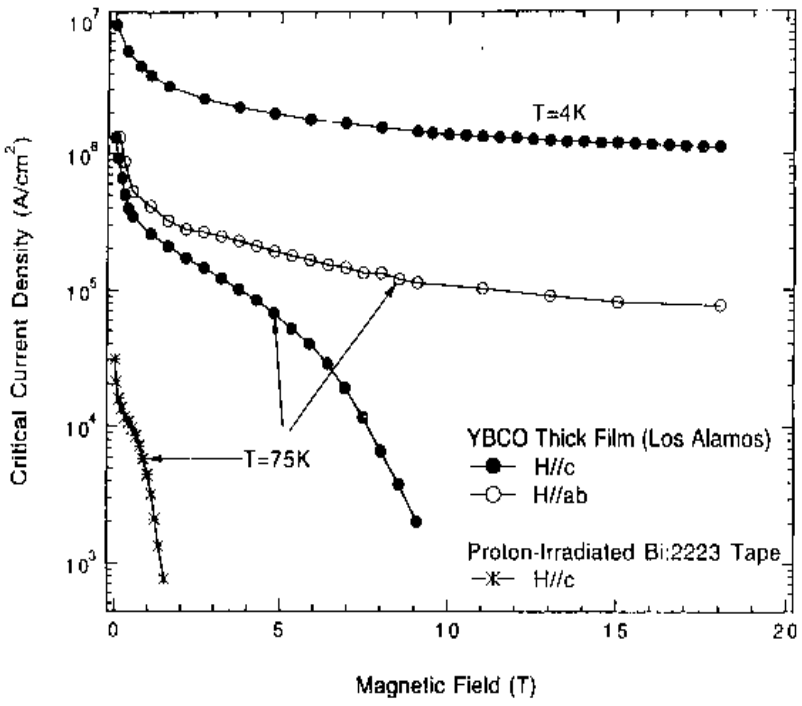

Figure 4 The critical current density for YBCO-123 as a function of magnetic field, for several temperatures and for different field orientation with respect to the crystal.

A large amount of anisotropy exists in the superconductor, depending whether the field is aligned with the c-axis or perpendicular to it. The difference is especially large at the higher temperatures. For YBCO thick film conductors, the c-axis is perpendicular to the tape.

An interesting alternative to the YBCO tapes is to use BSCCO material, 2212, not shown in the Figure. This material has good current carrying capabilities at low temperatures, and is easier to manufacture than YBCO [Herrmann].

d. SC Radiation damage

The radiation damage to high Tc and comparison to low Tc for fusion applications has been addressed previously. In this paper, only a brief summary is provided.

The limit of radiation damage to high Tc superconductors has not been established yet, with indications that properties improve through neutron fluences in excess of 3 x 10^{22} n/m^2. It is assumed that their limit is about 10^{23} n/m^2, about half and order of magnitude higher dose than that for low temperature superconductors. [Kupfer, Sauerzopf]

e. Nuclear and AC losses Heating

By operating at 50-77 K it is possible to remove the same thermal power by using a refrigerator that is ~40 times smaller than if the same thermal power is removed at 4 K. Therefore, neutron, gamma and AC loss heating of the cryogenic environment ceases to be a constraint for practical designs when high temperature superconductors are used.

The choice of operating temperature is important because it impacts the coolant choice. For temperatures lower than about 66 K, the only practical coolant is high pressure He gas. For higher temperatures, liquid nitrogen is the coolant of choice.

f. Cooling

For the low TC option, usual cooling techniques can be used (pool boiling, or Cable-in-Conduit Conductor), using liquid He.

In order to cool the elements in the quadrupole magnets that are manufactured with high Tc, alternatives to the use of a cryogenic fluid need to be developed. This is because there are not appropriate cooling liquids between liquid nitrogen and liquid helium. Hydrogen is undesirable because of explosion problems, and neon is very expensive, although available.

Dry systems can be developed which reduced the amount of liquid required. In order to remove the heat from the bulk of the magnet to the ends, it is possible to allocate a fraction of the cross section to a high-thermal conductivity element, used to conduct the heat to the ends of the quadrupoles, where it can be removed. It is necessary to use a non-structural element for this purpose, since the thermal conductivity of the structural elements is usually very small. Figure 4 shows an schematic of the cross section of one of the flat plates used in the cosine quadrupole array design, with edges made of highly conductive material (in this case assumed to be copper).

By utilizing this approach, assuming a volumetric heat load in the magnets of 1 mW/cm^3 and a length of the quadrupole of about 1 m, it is possible to decrease the temperature difference between the center of the magnet to the ends to about 2-3 K, with the use of only 5% of the cross sectional area for the copper. The temperature difference across the plates are substantially smaller than this.

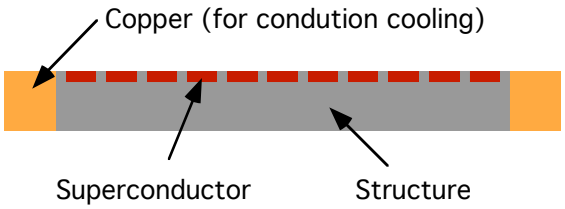

Figure 5. Illustrative approach for cooling bulk of plate, with high conductivity material at the edges of the plate.. Heat removal from plates occurs and the ends of the magnet

At the ends, the heat must be removed, either by high pressure Helium or by liquid neon.

IV. Quadrupole magnet implementation.

In this section, the rules and methods developed in the previous sections are used to illustrate the design options. Designs will be presented, for a low temperature material wound from conventional Rutherford cable conductor, and for high-Tc tape made with YBCO thick films. The goal is not to design the best magnet, but to illustrate the process.

It is assumed that the high-Tc magnet is a sine quadrupole arrangement, while the low Tc magnet is a cosine quadrupole arrangement. The bore of the magnet is the same, with the same field gradient. The goal is to determine the cell size required for the design.

Both designs have the same requirements: The parameters for the quadrupoles are as follows: a beam aperture of 0.15 m, the beam tube thickness is 0.001 m, the thickness of the MLI (cryogenic shielding) is 0.005m and the thickness of additional shielding/structure is 0.03 m. In addition, it is assumed that the conductor pack has a 0.005m thick structural envelope for ease of assembly and to help with buckling constrain and the axial loads. These thicknesses are directly between the superconductor elements and the beam aperture.

a. Low Tc cosine quadrupole magnet design

In the case of low-Tc magnet, it is not possible to manufacture the plates or the 90 degree angle elements using epitaxial techniques, and the superconductor needs to be wound in supporting structure. This limits the options for the manufacture of the flat plates (for cosine quadrupoles) or angle elements (for sine quadrupoles).

For the case of the cosine quadrupoles, because the loads result in tension in the flat plate structure if it is made continuous, the conductor needs to be supported by channels in the structure, if the flat plate elements are self-supporting. This makes the structure substantially less effective. It is possible to prevent large tensile stresses in the flat plates, as suggested in the force calculations section above, by place a slit through the middle of the plate and reacting the loads in one half of the plate to be supported by the adjacent plate, which has loads that are equal but opposite in direction. In this manner, the conductor and structure are in compression, and a substantial fraction of the load can be carried by the conductor in compression.

The unit cell is illustrated in Figure 6. The conductor is probably Rutherford cable, with react and wind technique (if the conductor is Nb_3Sn). The issue of winding at the ends, with tight radius, is beyond the scope of this paper. As mentioned above, the cosine quadrupole has a current distribution that varies linearly with distance from the center of the flat element. This can be

approximated by placing more conductors in regions away from the center of the flat element, as indicated in Figure 6. We mentioned above that the loads from the conductor are reacted by next-neighbor. In the illustration a positioning and load transferring structure is shown whose purpose is to transfer the loads from one flat element to the opposite one. Of course, each position and load transferring structure is associated with both on horizontal and vertical elements, as indicated in the picture. However, it is emphasized that the flat elements, as indicated in the picture, carry no net current. In other words, the elements behave different electrically and structurally (with currents not being shared, but loads being shared among separate elements).

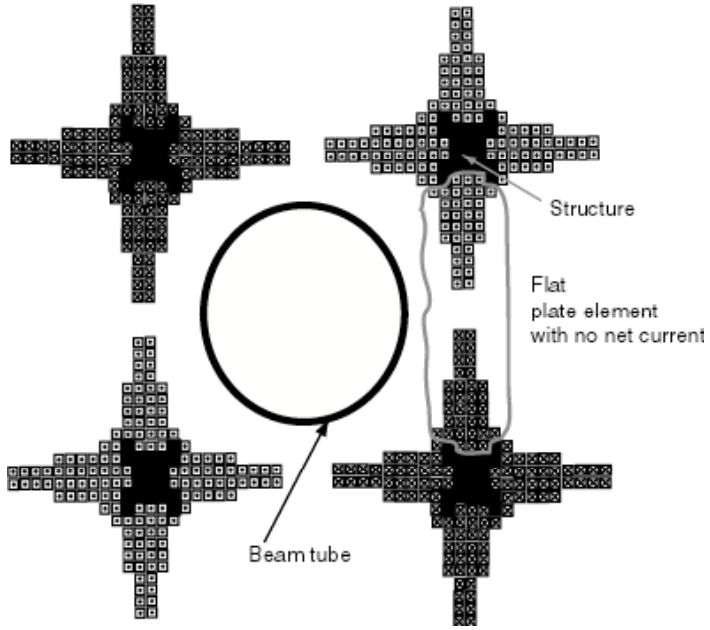

Figure 6. Illustrative diagram of cell for wound cosine quadrupoles (low Tc). Loads generated in opposite sides of plate elements are reacted by antisymmetric forces in adjacent plat element, not through structure in the plate element.

In the design of Figure 6, the current in the cross corner section is all in the same direction. This is unfortunate, in that it is not possible to assemble them as a unit prior to installing them in the array, but instead are made of elements that when put together form the cross corner assemblies

Several values of the field gradient have been used, from an aggressive of 40 T/m to a less aggressive of 20 T/m. note that the half-cell dimension a does not vary much with varying field gradient. This is because the bulk of the dimension between the beam channel and the cell symmetric plate is determined by constant values of shielding, shielding/structure, and tube diameter. The effect of the thickness of the superconductor is not very important, because the superconductor element is most thick in the region where the space is not needed for cryogenic insulation, radiation shielding or tube diameter, that is, in the region in the corner

of the cells. For the cases illustrated in Table 2 the assumed current density in the Nb_3Sn superconductor was chosen substantially smaller than what could be possible. It is assumed that the superconductor has a copper fraction of 50%, that the structure and cooling of the conductor decreases the average current density by an additional factor of 4, on top of a margin of 70% of current sharing. The current density was chosen so that the compressive stresses in the conductor, excluding the additional structure that can be provided by the shielding material, is around 200 MPa, to limit the strain degradation in the conductor. Indeed, it is possible to utilize NbTi for those cases in Table 2 with field gradients of 30 and 20 T/m.

Table 2

Cosine quadrupole using Nb_3Sn superconductor

Field gradient	T/m	40	30	20
a	m	0.197	0.193	0.191
Bmax	T	7.9	5.8	3.8
A	T/m	20	15	10
Current density	A/m^2	2.6E+08	3.8E+08	5.4E+08
Current density, non-copper	A/m^2	3.0E+09	4.3E+09	6.2E+09
Superconductor current density, max (K)	A/m	1.25E+07	9.22E+06	6.08E+06
Total conductor thickness	m	4.85E-02	2.43E-02	1.12E-02
Compressive stress in conductor	Mpa	2.01E+02	2.12E+02	1.98E+02
beam radius	m	0.15	0.15	0.15
Field at aperture	T	6.0	4.5	3.0
Conductor cross section	m	0.003	0.0025	0.002
Pack current	kA	2.3	2.4	2.2
number of layers, max		16	10	6
number of turns per layer, max		131	154	191
Stored energy per unit length	MJ/m	2.56	1.32	0.56

The cells that are at the edge of the array need compensation in order to behave in the manner described here. This is accomplished by placing appropriate current distribution in this region in order to simulate the presence of an infinite array of quadrupoles. The current distribution at the edge of the quadrupole array for achieving this effect has been calculated in the past by Thome. [Thome]

For the case of a cosine quadrupole magnet using high Tc materials, the conductor distribution in the plate elements is shown in Figure 7. This figure illustrates the options for depositing the material for the cosine quad arrays that requires non-uniform current distribution in the plates. The current distribution, which flows anti-symmetrically on opposite side of the plate, can be made by applying a constant thickness conductor with varying spacing, or it can be done with relatively constant spacing but with varying width, or a combination of the two. The current sharing density is relatively uniform, since the magnetic field is uniform across the plate.

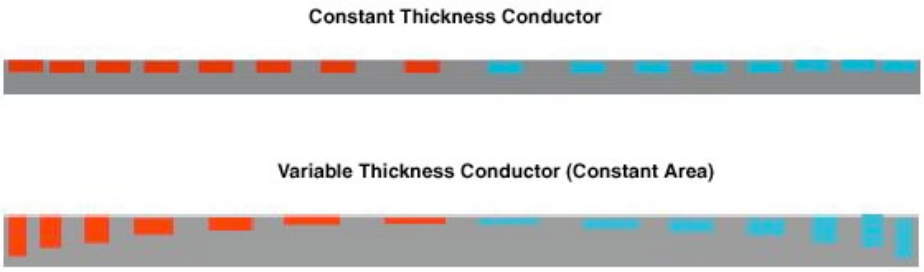

Figure 7. Design of plates using epitaxially deposited high Tc superconductor for cosine quads arrays.

b. High Tc sine quadrupole magnet.

For the case of the sine quadrupoles arrays, the conductor needs to be placed or deposited on 90 degree angle elements, with uniform current density. The loads from the axial conductor are aligned with the plates, but point towards the middle of the plates, as described above in the force calculation section. Not only is there conductor in the cells midplane but the forces are greatest there, requiring most support in the region that most affects the beam radius. The most efficient method of supporting these loads is in compression, in therefore means need to be provided to control buckling.

In this section, illustrative design parameters of a sine magnet with high Tc are presented. The main beam parameters (field gradient, beam aperture and thicknesses) are the same as for the low Tc magnet described above. The superconductor is now spaced uniformly in the structural 90-degree angles. The loads are supported by compression in the planes that make the half angle, and as before, a 0.005 m structure is used to surround the superconductor pack to ease handling and to address axial loads and buckling.

Table 3 shows results from the calculations for field gradients similar to those in Table 2 for low Tc. It should be noted the cell size is not changed much from one design to the other. The cell size in this case is larger not because of the use of high Tc material, but because of the use of the sine quadrupole arrangement. But in either case the cell size is on the order of 0.40 m (full size)

Figure 8 shows a schematic diagram of one of the 90-degree angle elements with high Tc superconductor material. The ends of the element need to be rounded to allow for current transfer from one plane of the angle element to the other.

Table 3

Illustrative designs of high Tc sine quadrupole magnet array

Field gradient	T/m	40	30	20
a	m	0.209	0.193	0.192
Bmax	T	8.4	5.8	3.8
A	T/m	20	15	10
Current density	A/m^2	2.1E+09	2.1E+09	2.1E+09
Current density, non-copper	A/m^2	3.0E+09	3.0E+09	3.0E+09
Surface current density, max (K)	A/m	1.33E+07	9.22E+06	6.11E+06
Total conductor thickness	m	6.34E-03	4.39E-03	2.91E-03
thickness of structure	m	2.32E-02	1.03E-02	4.51E-03
beam radius	m	0.150	0.150	0.150
Field at aperture	T	6.0	4.5	3.0
SC parameters				
Conductor thickness	m	0.00005	0.00005	0.00005
Pack current	kA	1.1	1.1	1.1
number of layers, max		127	88	58
number of turns per layer, max		42	39	38
Stored energy per unit length	MJ/m	3.24	1.32	0.58

Figure 9. Schematic diagram of a 90-degree element of a sine quadrupole magnet using high Tc superconductor

An advantage of this design over the cosine quadrupole one is that the corner elements can be assembled remotely and inserted, due to the zero net current of these elements. This is not possible with the sine quadrupole elements, since the current carried by the elements in a corner section is all in the same direction (see Figure 8)

V. Comments on end fields

Using the same approach as above to calculate the magnetic field away from the ends of the quadrupole array, it is possible to calculate the fields in the ends. Using the same symmetry arguments, the scalar potential that described the end fields is given by

$$\Phi = \sum_{ij} \sin(k_x x) \sin(k_y y) \exp(-(k_x+k_y) z)$$

where the sum if over i,j, where $k_x a = \pi i$ and $k_y a = \pi j$. Quadrupole like fields are given by i=j=1, in which case the field has mainly cos(2θ) component. By appropriately choosing the current density at the quadrupole ends it is possible to avoid generation of fields that are not quadrupole like. The forces, by symmetry, are still aligned to the planes between cells.

The lowest harmonic (with i = j = 1) generates more than the fundamental poloidal harmonic, as described above. The first four harmonics (n = 2, n = 4, n = 8,) are shown in Figure 10. Note that n = 6 is not shown since it is 0 because of symmetry.

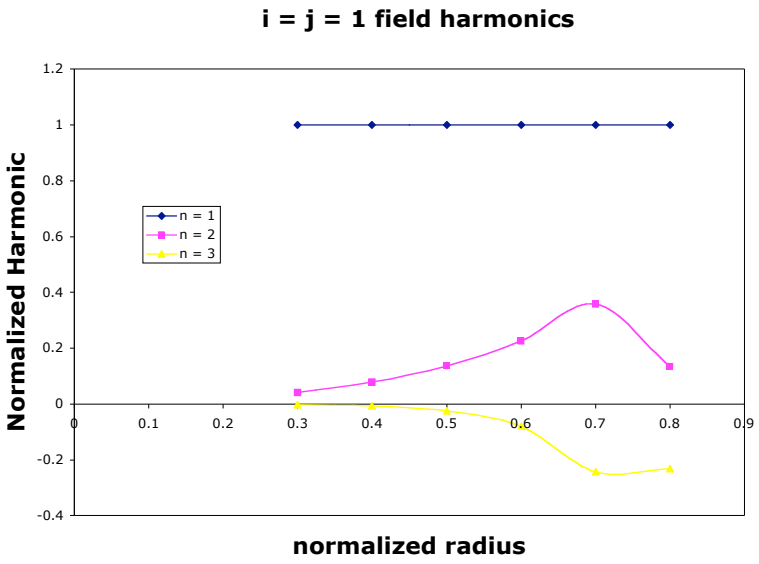

Figure 10. Normalized field poloidal harmonics that correspond to i = j = 1, as a function of the normalized radius.

Since different harmonics (with $i \neq 1$, and/or $j \neq 1$) have different decay rates (in the z direction) than the i = j = 1 case, it is not possible to zero out those undesirable harmonics they way their were cancelled in the middle of the array. It is difficult to converse the field purity in the ends. The contributions to the field errors by the ends of the quadrupoles need to be minized.

VI. Magnet costing of epitaxially made magnets

The unit-cost of the quadrupole magnets may be substantially decreased by utilizing the epitaxial manufacturing design described above. Instead of the complex manufacturing processes used for today's LTS magnets, modern rapid-prototyping techniques could be used [Waganer]. The flat plates or 90 degree angle elements can be manufactured from either powders (as in the ARIES-ST reactor) or from raw stock. They can then be coated with the different layers to manufacture the superconductor, in a process similar to that used in printed circuits and that is very easily automated. Presently Ni is being used as the substrate for tapes. It is not clear whether Inconels (Ni-based steels) could be used instead. If not, then the steel would have to be coated with a layer that serves as a diffusion barrier, onto which Ni is deposited. Alternatively, tapes can be used, which after they are manufactured can be soldered onto the structural plates. However, the use of tapes may increase the cost of the magnet, due to increased number of processes involved. Figure 11 shows a picture of a set of superconductor patterns on silver, as reported by Bromberg [Bromberg 95].

It is estimated that the cost of the superconductor is on the order of $200/kg, which comparable to NbTi, but is cheaper than Nb_3Sn. Since the superconductor is such a small fraction of the cross sectional area, the cost of the magnets will be determined by the cost of the structure. The cost of the structure is being determined. It is being assumed that modern manufacturing techniques will be used. Cost as low as $50/kg for the magnet could be feasible. [Masur]

The use of epitaxial methods of fabricating the magnet allows great flexibility in the choice of the cross section of the magnet and may help address those issues that were not discussed in this paper, such as the ends of the quadrupoles.

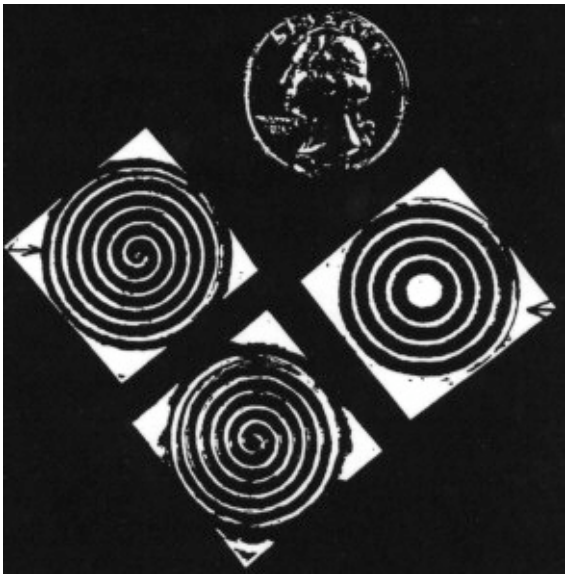

Figure 11. Single sided samples made of BSCCO 2212 applied on a squared-silver substrate. An American quarter dollar is shown for comparison.

VII. Summary and Conclusions

The design of quadrupole arrays for the final focusing magnets for the Heavy Ion Driver for inertial fusion has been scoped. Options for topology that use the fact that the quadrupoles are arranged in an array have been investigated, and it has been determined that important difference occur between single quadrupole designs and quadrupole array designs. The two types of possible magnets have been evaluated, using both high Tc and low Tc. High field purity can be achieved with these topologies. The purpose of the paper is not to develop a fully optimized, complete design, but rather to scope the options for the magnets.

The use of high Tc materials may be enabling technology that spur qualitative changes in the manufacturing of quadrupole magnets arrays.

Acknowledgment

This work was supported by US Department of Energy, Office of Fusion Energy Science.

References

[Bromberg 01] Bromberg,-L.; Tekula,-M.; El-Guebaly,-L.-A.; Miller,-R and the ARIES team, *Options for the use of high temperature superconductor in tokamak fusion reactor designs*, *Fusion-Engineering-and-Design* **54**(2): 167-80 (2001)

[Bromberg 91] L. Bromberg, P. Titus, and J.E.C. Williams, *Nested Shell Superconducting Magnet Design*, in *Proceedings of the 14th IEEE/NPSS Symposium of Fusion Engineering*, 319 (San Diego, Ca, Oct 1991)

[Bromberg, 94] Bromberg L, Williams JEC, Tekula MS. *High Tc Bitter magnets*. IEEE *Transactions on Magnetics*.**30** 1687-92 (1994)

[Bromberg 95] Bromberg, L., M. Sidorov, R. Mints and T. Holesinger, *Electrical and thermal behavior of patterned superconducting disks*, *IEEE Transactions on Applied Superconductivity* **5** 321-4 (1995)

[Kupfer] H. Küpfer et al: Z. Phys. B 69 (1987) 167-171

[Thome] Thome, R., MIT Plasma Science and Fusion Center private communication (2001)

[Maley] Maley, M.P. *et al., Optimization of Transport critical current in HTS Conductors*, in *1996 Annual Peer Review Meeting, U.S. Department of Energy*, Washington D.C. (July 31, 1996).

[Sauerzopf] F.M. Sauerzopf et al.: PRB 51 (1995) 6002-6012.

[Sawh] Sawh R-P, Ren Y, Weinstein R, Hennig W, Nemoto T. *Uranium chemistry and pinning centers in high temperature superconductor*. *Physica C*, **305**, no.3-4, pp.159-166, 1 Sept. 1998.

[Waganer 99] Waganer, L.M. *Ultra-Low Cost Coil Fabrication Approachh for ARIES-ST*, paper submitted to *Fusion Engineering and Design*, Jan 1999

[Schultz] *,* J.H. Schultz, *Integration of High-Tc Superconductors into the Fusion Magnet Program* MIT Plasma Science and Fusion Center report PSFC Report: PSFC/RR-99-5 (March 23, 1999); http://www.psfc.mit.edu/library/99rr/99rr005/99rr005_abs.html

[Masur] Masur,-L.-J., Kellers,-J., Feng-Li, *et al*., *Industrial high temperature superconductors: perspectives and milestones*, *IEEE-Transactions-on-Applied-Superconductivity* **12** 1145-50 (2002)

[Meinke] *Development of quadrupole arrays for heavy-ion fusion,* Meinke, R. B., Faltens, A., Bangerter, R. O., Scanlan, R. M., Seidl, P, *Transactions-on-Applied-Superconductivit* **10**: 192-5 (2000)

[Herrmann] Herrmann,-P.-F., Allais,-A., Bock,-J., *et al. BSCCO based superconductors for magnet applications*, *In Advances-in-Superconductivity-XII.-Proceedings-of-the-12th-International-Symposium-on-Superconductivity-ISS'99* 730-5 (2000)

[Iijima] Iijima,-Y.; Matsumoto,-K., *High-temperature-superconductor coated conductors: technical progress in Japan, Superconductor-Science-&-Technology* **13** 68-81 (2000)

[quadrupole] Rago,-C.-E., Spencer,-C.-M., Wolf,-Z. and Yocky,-G., *High reliability prototype quadrupole for the Next Linear Collider*, *IEEE-Transactions-on-Applied-Superconductivity* **12** 270-3 (2002)

[OGITSU] Ogitsu,-T., Nakamoto,-T., Ohuchi,-N., *et al., Status of the LHC low-beta insertion quadrupole magnet development at KEK, IEEE-Transactions-on-Applied-Superconductivity*; **12** 183-7 (2002)

[SIMON] Simon,-F., Gourdin,-C., Schild,-T., *et al., Test results of the third LHC main quadrupole magnet prototype at CEA/Saclay*, *IEEE-Transactions-on-Applied-Superconductivity*. **12** 266-9 (2002)

[Devred] Devred,-A., Durante,-M., Gourdin,-C., Juster,-F.-P., *et al. Development of a Nb/sub 3/Sn quadrupole magnet model, IEEE-Transactions-on-Applied-Superconductivity.* **11** 2184-7 (2001)

[Zhang] Zhang,-W.-W.; Bernal,-S.; Li,-H.; Godlove,-T.; *et al. Design and field measurements of printed-circuit quadrupoles and dipoles*, *Physical-Review*-Special-Topics-Accelerators-and-Beams **3** 12 (2000)

[Faltens] Faltens,-A. and Shuman,-D., *A superconducting quadrupole array for transport of multiple high current beams*, presented at the *18th-IEEE/NPSS-Symposium-on-Fusion-Engineering*.-IEEE Symposium-Proceedings-Cat.-No.99CH37050, ppp 362-6 (1999)

[Bittner] K. Bittner-Rohrhofer, P. Rosenkranz, K. Humer, H.W. Weber, J.A. Rice, P.E. Fabian and N.A. Munshi, *Characterization of reactor irradiated, organic and inorganic hybrid insulation systems for fusion magnets*, *2001 Joint Cryogenic Engineering Conference and International Cryogenic Materials Conference*. 16-20 July 2001 Madison, WI

[Chapiro] Chapiro, A., Clough, R., Mermilliod, N. and Tavlet, M, *What is ageing? Are there still problem to be solved?, Nucl. Instr Meth. Phys. Res* **B** 131 x-xii (1991)